



Research Article

ISSN : 0975-7384
CODEN(USA) : JCPRC5

New tricks for an old dog: discovery, synthesis, *in vitro* and *in vivo* antitumor evaluation as well as docking studies of novel rutaecarpine derivatives as Topoisomerase I inhibitors

Yingjie Zhang^{a*}, Jianying Xu^a, Yuankun Zhang^a, Lu Jia^b and Guanghui Liu^c

^aDepartment of Chinese Medicine, Zhengzhou People's Hospital, Zhengzhou, P. R. China

^bSchool of Pharmacy, Zhengzhou University, Zhengzhou, P. R. China

^cFirst Affiliated Hospital of Zhengzhou University, Zhengzhou, P. R. China

ABSTRACT

DNA Topoisomerase I (TopI) is over-expressed in tumor cells and is an clinical important target for a variety of cancer chemotherapies. Herein, we have identified the antiproliferative activity of some sulphonic acid esters derived from rutaecarpine as well as 5-methylene rutaecarpine, for the purpose of improving therapeutic benefits of camptothecin and evodiamine. The synthesized N¹³-substituted rutaecarpine compounds were evaluated for their *in vitro* cytotoxicity against A549, HepG-2, U251, HeLa and MCF-7 human carcinoma cell lines by MTT assay, of which the hit **3d** exhibited potent anti-tumor activities on all cell lines. Additionally, **3d** was found to inhibit substantially the tumor growth on the HepS-bearing mice at a dose of 80 mg/kg. Subsequently, preliminary structure-activity relationship was explored based on the combination of biological data and ligand-based molecular modeling methods, which could provide guidance for designing new analogues of rutaecarpine. Finally, *in silico* screening studies of sulfonic rutaecarpine esters revealed that they could form hydrogen-bonding and hydrophobic interactions with several amino acid residues of topoisomerase I at the cleavage site, resembling the binding format between camptothecin and topoisomerase I-DNA complex.

Keywords: Rutaecarpine; topoisomerase I inhibitor; antitumor; *in vitro* and *in vivo*; *in silico* screening;

INTRODUCTION

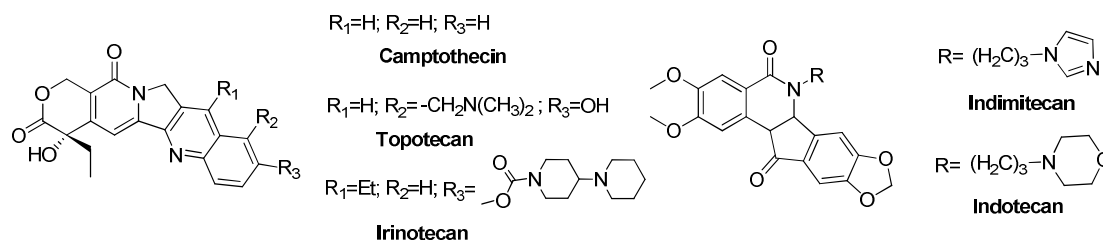
Topoisomerase I (TopoI) is an essential and ubiquitous enzyme for DNA replication, chromosome condensation and chromosome segregation^[1]. As the validated target for the treatment of human cancers, TopoI could be inhibited by camptothecin and many other structurally diverse compounds. Among these inhibitors of TopoI, the cytotoxic quinoline alkaloid camptothecin (CPT) showed promising anticancer activity in previously clinical trials. However, the instability of the structurally essential lactone ring and adverse drug reaction restricted its application^[2]. Improvably, topotecan was approved for the treatment of ovarian and lung cancer^[3]. Another camptothecin derivative irinotecan was ratified for the treatment of colon cancer^[4] (Fig.1).

Although CPT derivatives are the only clinically approved TopoI inhibitors, they have a number of major drawbacks: 1) Conspicuous instability to carboxylate form in blood^[5], 2) rapid reversal of the trapped cleavable complex after drug removal, requiring repeated infusions^[6], 3) resistance of cancer cells over-expressing membrane transporters^[7], and 4) adverse effects such as vomiting, diarrhea and neutropenia, which restrict the dose that can be safely administered^[8]. Moreover, several resistance mutations of TopoI (such as Asn722S and Arg364H) have been reported^[9].

Therefore, medicinal chemists have developed numerous non-CPT derivatives to circumvent these disadvantages. Indotecan and indimitecan^[10], two indeno[1,2-c]isoquinolin-5,11-diones are presently under evaluation in a Phase I

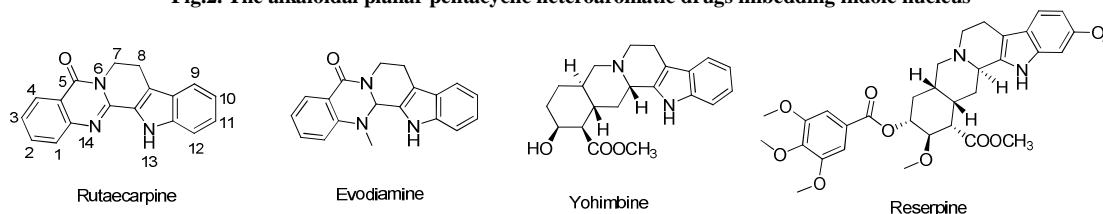
clinical trial treating with relapsed solid tumors and lymphomas. All these chemicals share linear flat polyaromatic drug chromophore, which form and stabilize the cleavable ternary drug–DNA–enzyme complexes that induce lethal DNA strand breaks, primarily by preventing the relegation step. Ultimately, this DNA-damaging effect leads to programmed cell death (apoptosis).

Fig.1. Some of the top-selling CPT topoisomerase I inhibitors



At the meantime, the planar pentacyclic heteroaromatic structures bearing indole nucleus are frequently found in many alkaloidal drugs showing diverse biological activities, for instance, Yohimbine^[11] (remedy of sexual dysfunction) and Reserpine^[12] (antihypertensive medicine). Rutaecarpine and Evodiamine^[13] (Fig.2.) are two major alkaloids isolated from *Evodia fructus* (Chinese herbal drug named Wu-Chu-Yu), which possess diverse biological functions such as anti-inflammatory^[14], antiproliferative^[15], antimetastatic^[16], vasorelaxant^[17] effect and apoptotic^[18] activities. Specifically, former researches have shown that rutaecarpine had dramatic inhibitory activity on carcinomatos^[19]. Molecular pharmacological basis for the ability of evodiamine to suppress proliferation, induce apoptosis, and inhibit metastasis can be concluded as follows: 1) evodiamine and rutaecarpine induced NF- κ B activation and NF- κ B-regulated gene expression^[20], 2) rutaecarpine inhibited the growth of LNCaP (prostate cancer cell line) through an accumulation of cell cycle arrest at G2/M phase and an induction of apoptosis^[21], 3) as high androgen levels accelerated the generation and growth of prostate cancer, evodiamine and rutaecarpine could prevent and treat prostate excrescence by down-regulation testosterone secretion based on reducing activity of cAMP-related pathways and 17 β -hydroxysteroid dehydrogenase (17 β -HSD)^[22], 4) evodiamine could also ignite autophagy^[23]. Recently, evodiamine has emerged as a promising TopoI inhibitor with uncommon “L type” conformation compared with the planar hit (e.g. camptothecin)^[24]. The sufficient understanding of TopoI’s molecular structure and mechanism of action also provides insights into the physiological functions of TopoI and a solid structural basis for the rational design of highly potent non-CPT TopoI inhibitors.

Fig.2. The alkaloidal planar pentacyclic heteroaromatic drugs imbedding indole nucleus

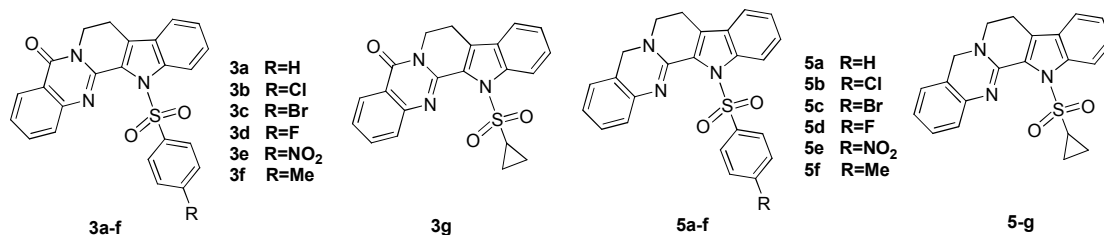


From the structural point of view, the indole N-H of rutaecarpine is a good functional group for the readily synthesis of various derivatives. The revealed docking model indicated that evodiamine only partly intercalated into the DNA base pairs and the attachment of an aromatic group to the indole N-H could improve its π - π stacking interactions with TopoI (e.g. N-benzoyl evodiamine derivatives)^[24].

With our continuous interest in the relationship between planar heteroaromatic molecule containing indole moiety and their biological activities and attempt to search for potential antitumor agents^[25], we initiated a project to design and develop the rutaecarpine-based new chemical entities towards the elevation of solubility, bioavailability and biological activity. Herein, we report the synthesis and cytotoxicity assay of some sulphonic acid esters of rutaecarpine as well as 5-methylene rutaecarpine.

On the other hand, molecular docking continues to hold great promise in the field of computer-based drug design, which screens small molecules by orienting and scoring them in the binding site of a target protein. Additionally, the synthesized compounds were subjected to molecular docking simulations to find out the potential molecular binding affinity and at the same moment further support the experimental cytotoxic tests. We performed our docking study with Discovery Studio Modeling 2.1 program (Accelrys Inc., San Diego, CA) on a Linux environment.

Fig.3. Design of compounds 3a-3g, 5a-5g

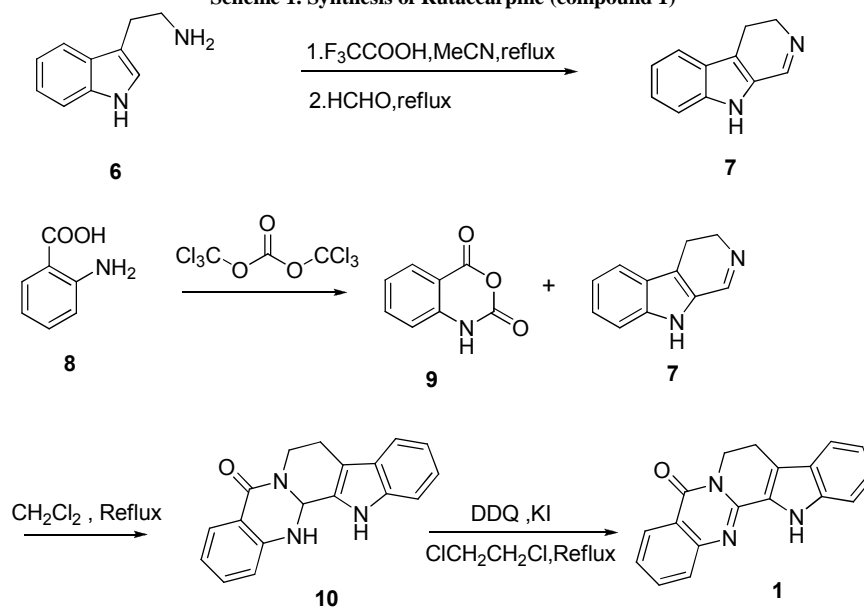
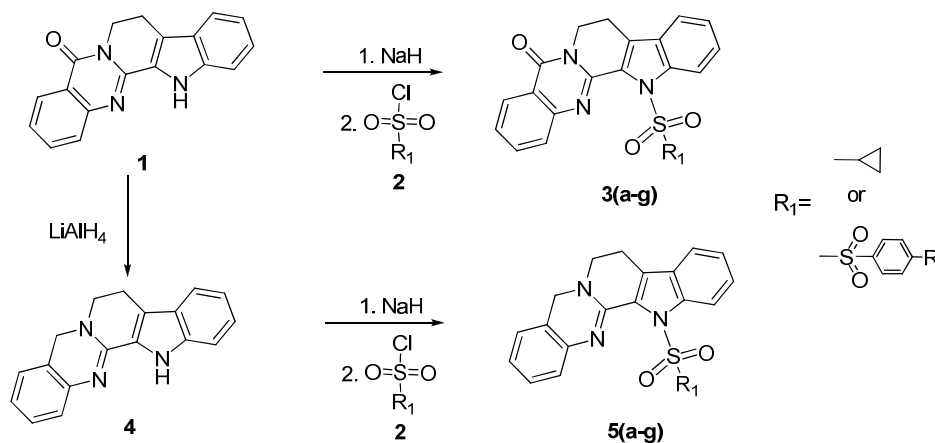


RESULTS AND DISCUSSION

2.1. Chemistry

2.1.1. General Procedure for the Preparation of **1** and **4**

Rutaecarpine was synthesized by an improved procedure from the synthesis of evodiamine (Scheme 1)^[26]. Starting from tryptamine **6**, **6** underwent ring closure after condensation with formaldehyde to form the Pictet–Spengler product **7** by acidic catalyst trifluoroacetic acid. Concurrently, in the presence of triphosgene, the key intermediate isatoic anhydride **9** was obtained by cyclization of anthranilic acid **8**, followed by the condensation with **7** affording intermediate **10**. Rutaecarpine was thus formed by DDQ oxidation of **10**. Rutaecarpine was treated with LiAlH₄ to afford the hydrogenated compound **4**.

Scheme 1. Synthesis of Rutaecarpine (compound **1**)Scheme 2. Synthesis of targeted compounds **3** and **5**

2.1.2. General Procedure for the Preparation of **3a–3g** and **5a–5g**

In the presence of NaH and DMF, compounds **3a–3g** and **5a–5g** were prepared by treating rutaecarpine **1** or hydrogenated rutaecarpine **4** with various sulphonyl chloride reagents (substituted benzenesulfonyl chloride and cyclopropanesulfonyl chloride) at room temperature (Scheme 2). After 3–5 h, the reaction mixture was washed with water and saturated NaCl solution sequentially, dried over desiccant, and concentrated in vacuo. The crude products were purified by column chromatography to give the targeted compounds.

2.2. Anti-proliferative activity *in vitro*

To evaluate the effects of the rutaecarpine and 5-methylene rutaecarpine derivatives on proliferation of human cancer cells, five cancer cell lines including A549, HepG2, U251, HeLa and MCF-7 were treated with various concentrations of tested compounds for 48 h using the MTT assay. The 50% inhibitory concentration (IC_{50}) was detected. As shown in Table 1, after sulfonylation with sulphonyl chloride reagents, most of the synthesized compounds showed better anti-tumor activities than those of the starting materials **1** and **4**. Specifically, compounds **3d** and **3e** exhibited more potent anti-tumor activities than rutaecarpine on all cell lines. The MCF-7 cells presenting the lowest IC_{50} were the most sensitive cells. It has been noticed that compounds **3d** and **3e** have similar structures, however, the compound **3d** showed better anti-tumor activities against four cell lines than compound **3e**. This preliminary structure-activity relationship patterns suggested that N- para substituted benzenesulfonylation of rutaecarpine played a significant role in their anti-tumor activities. Both compounds **3d** and **3e** exhibited potent activities against the MCF-7 cell line with IC_{50} values of 2.68 μ M and 5.84 μ M, respectively, while compounds **3a** (IC_{50} =5.23 μ M) and **3e** (IC_{50} =9.45 μ M) presented good activities against HepG-2 cell, as well as compound **3b** displayed potent activity against A549 cell line with an IC_{50} value of 4.63 μ M.

Table 1. IC_{50} values of the tested compounds against five human tumor cell lines^a

Compd.	IC_{50} (μ M)				
	A549	HepG-2	U251	HeLa	MCF-7
1	25.88±1.56	55.66±2.25	20.13±1.05	37.63±1.57	8.40±0.17
3a	63.87±1.74	5.23±0.84	29.00±0.21	>100 ^a	5.72±0.12
3b	4.63±0.13	>100	>100	37.17±0.39	8.96±0.24
3c	38.33±2.31	25.29±1.28	22.76±1.03	47.85±2.56	6.32±0.33
3d	5.54±0.85	9.45±0.81	11.72±0.45	18.42±1.71	2.68±0.22
3e	11.27±0.08	15.81±0.54	21.65±1.28	14.26±4.52	5.84±0.78
3f	14.12±0.10	13.99±0.18	27.83±1.37	>100	7.13±0.28
3g	16.29±0.17	>100	>100	72.84±1.39	13.81±0.14
4	11.12±0.10	58.39±1.82	23.71±1.50	>100	89.13±3.27
5a	18.29±0.17	67.32±2.67	67.12±3.28	32.38±1.02	63.88±2.02
5b	10.43±0.21	>100	>100	>100	>100
5c	14.29±0.37	87.69±0.80	>100	88.11±1.73	79.87±1.03
5d	>100	7.49±0.24	>100	>100	43.87±2.09
5e	>100	49.33±0.87	>100	74.98±2.74	>100
5f	19.74±0.98	8.14±0.31	6.98±0.34	17.63±0.29	22.40±1.07
5g	12.79±0.21	4.92±0.10	3.41±0.1	64.93±0.29	35.72±0.82
CPT	14.56±0.61	24.65±1.87	12.35±0.41	11.41±0.89	8.59±0.37

^a Data are presented as means±S.D. (n = 3). $IC_{50} > 100 \mu$ M. The maximal concentration of tested compounds is 100 μ M. When $IC_{50} > 100 \mu$ M, we regarded the compounds' anti-tumor activities were too weak to have further research. It is worth to note rutaecarpine, which has been recognized as a potential chemotherapeutic agent, is the standard as well as CPT in five cell lines test.

Among the tested compounds, the series **5a–5g** showed higher IC_{50} values than the parallel compounds **3a–3g**. It seems that the conversion of the C⁵-carbonyl to methylene would decrease the antiproliferative activities of 5-methylene rutaecarpine compounds in contrast to their corresponding prototypes. Comparing the IC_{50} values of the compounds **3a–3f** with that of **3g** in different cell lines, aromatic sulphonic acid esters were found to exhibit more potent activity than alkyl sulphonic acid ester **3g**. The IC_{50} values decreased dramatically when R was fluorine, and stronger anti-proliferative activity was observed for **3d** than those of halogen (**3b–3c**) and nitro **3e** substituents correspondingly. This suggested that, among all target compounds, compound **3e** exhibited the most potent anti-tumor activity against tested cell lines: IC_{50} values of 5.54 μ M against A549, 9.45 μ M against HepG-2, and 2.68 μ M against MCF-7 (stronger than parent rutaecarpine of 8.40 μ M and positive control CPT of 3.65 μ M). Further structural modification based on present SAR and more intensive biological studies were now being undertaken in our lab.

2.3. *In vivo* antitumor assessment with the HepS xenograft

We investigated the effect of **3d** treatment on tumor growth using HepS xenografts. As indicated in Table 2, there was not a gross growth inhibition toward the **3d** treated mice, in fact, the body weights of the tumor-bearing mice treated with **3d** had a fairly profound increase as compared to the control group, i.e. 7.1 g (20 mg/kg of **3d**), 6.5 g (40 mg/kg of **3d**) and 6.1 g (80 mg/kg of **3d**) versus 5.2 g (control). On the contrary, the body weights of the tumor-bearing mice treated with camptothecin (CPT, 20 mg/kg) increased only by 4.3 g.

However, compound **3d** treatment resulted in a significant attenuation in the tumor weight in a dose-dependent manner. In specific, a 68.55% reduction in the tumor weight was achieved following **3d** treatment (40 mg/kg), whereas CPT treatment (20 mg/kg) only afforded a 47.06% tumor weight reduction (Table 2). The *in vivo* antitumor efficacy of **3d** was consistent with its *in vitro* cytotoxicity. Furthermore, mice treated with **3d** showed improved index of thymus and spleen than those treated with CPT. Therefore, it appears that **3d** possessed stronger antitumor efficacy and less side-effect than CPT in the HepS tumor model.

Table 2. The inhibitory effect of 3d on HepS tumor xenograft (Mean \pm S.D.) (n = 10)

Group	Dose (mg/kg)	Weight(g)		Inhibitory rate	Thymus index(mg/g)	Spleen index(mg/g)
		Before treatment	After treatment			
control	–	21.51 \pm 1.15	26.71 \pm 1.15	–	2.31 \pm 0.43	6.71 \pm 1.06
3d	20	21.29 \pm 1.33	28.40 \pm 1.38	29.13%	2.16 \pm 0.74 ^a	9.12 \pm 0.88 ^a
3d	40	21.45 \pm 1.28	27.95 \pm 1.27	42.40%	2.58 \pm 0.51 ^a	9.37 \pm 1.10 ^a
3d	80	21.76 \pm 1.47	27.87 \pm 1.33	68.55%	2.75 \pm 0.68 ^{a*}	10.13 \pm 1.27 ^{a*}
CPT	20	21.37 \pm 1.39	25.66 \pm 1.14	47.06%	1.35 \pm 0.47	5.17 \pm 0.93

^a Significantly different from CPT group at $p < 0.01$; * significantly different from control group at $p < 0.05$;

2.4. Molecular docking

In silico approaches are routinely and extensively used to reduce the cost and time for drug discovery. Several commercial and academic softwares are available for molecular modeling and docking studies. Our objective of employing molecular docking programs is to predict the correct placement of new synthesized molecules within the binding pocket of enzyme. Herein, as all of 16 molecules were satisfied with Lipinski's drug properties, docking was performed against to the active site of crystal TopoI-DNA-CPT complex (PDB code 1T8I) by commercially available Discovery Studio Modeling 2.1 program (D.S. 2.1).

The first step of the study was to evaluate the reliability of D.S. 2.1 program for the prediction of the binding pose of TopoI inhibitors into the crystal structure of the protein. Following a well-accepted approach, CPT and Topotecan were docked into the crystal structure (PDB code 1T8I) through D.S. 2.1, The docking reliability was evaluated through a comparison of the root-mean-square deviation (RMSD) between the positions of heavy atoms of the ligand in the calculated and experimental structures found docked positions of the ligand and the experimental ones. Utilizing the average RMSD value as a measure of the reliability of the methods applied, the D.S. 2.1 software with LigandFit fitness function seemed to be the most suitable one. It gave the best results with the average RMSD value 1.43 Å (lower than 2.0 Å). Therefore, LigandFit fitness function was selected for the virtual screening study.

Their interaction energies were calculated using the scoring functions to estimate the ligand-binding energies. Other input parameters for docking were set as default options. Thus, binding sites were defined based on the ligands already present in the PDB files which were followed by site sphere definition. Dock scores were calculated from the energy level conformations of the TopoI inhibitor complexes. A higher score indicates a stronger receptor-ligand binding affinity.

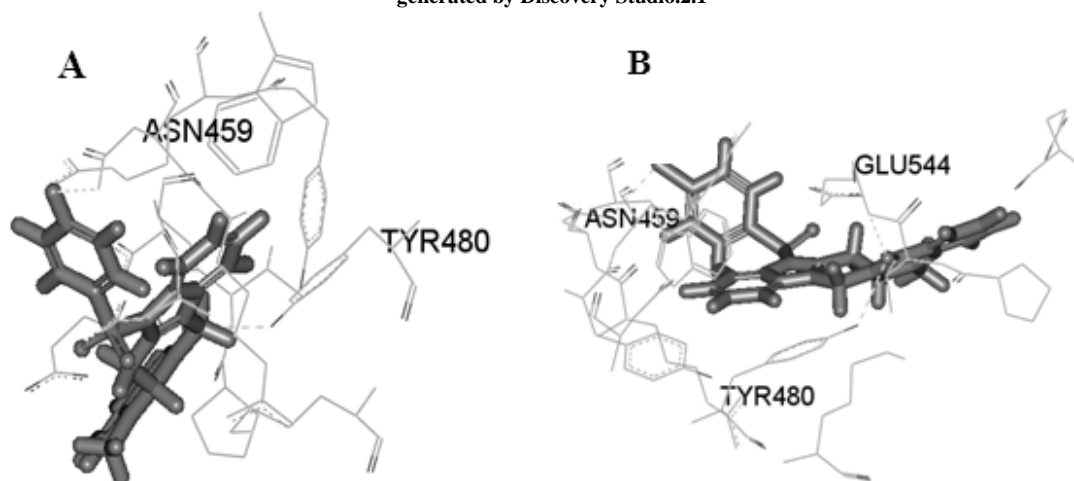
Table 3. Hydrogen bond interactions between the DNA TopoI and the compounds (Results were analysed using H-bond monitor of Discovery Studio.2.1)

Compound	-PLP1	-PLP2	Dock score	Inter-molecular H-bonds	Ei
1	53.67	55.79	67.9514	TYR480-O22	101.741
3a	77.16	78.31	89.5647	TYR480, GLU544-O22	121.382
3b	81.34	79.45	88.8466	TYR480, GLU544,(ASN459-C133)	119.483
3c	78.26	77.92	88.4731	TYR480, (ASN459-Br33)	120.353
3d	76.92	79.01	89.1361	TYR480, GLU544, (ASN459-F33)	119.416
3e	81.12	78.56	88.1785	TYR480	120.353
3f	79.36	80.11	88.6322	TYR480	119.934
3g	79.71	78.53	77.7094	TYR480	117.965
4	–	–	–	None	–
5a-5g	–	–	–	None	–

All compounds were employed for docking study toward TopoI, and the result showed **1** and **3a-3g** had high binding affinity with the target. In contrast, no binding was observed for ligands (**4** and **5a-5g**) with the important residues of TopoI (i.e. TYR480, GLU544 and ASN459), since there was no hydrogen bond between them. Table 2 listed the different score values of top ranked ligands. As shown in Table 2, the dock scores of the compounds **3a-3g** were observed better than that of rutaecarpine, which were in good accordance with their cytotoxicity test. Particularly, **3a** and **3d** had maximum scores of 89.5647 and 89.1361, which were in agreement with their intermolecular H-bonds, that is to say **3c** formed two hydrogen bonds with TopoI as well as **3a** formed three. Compound **3e** had comparable dock score of 88.1785, but it exhibited satisfactory result in cytotoxicity test (Table 1). In this study, all of the seven compounds (series **3a-3g**) were shown the favorable drug likeness property. Further studies will be

concentrated to verify these results with *in-vivo* confirmation.

Fig. 4. Binding mode and docked conformations of selected 3b(A) and 3d(B) in the active site of TopoI-DNA complex. The figure was generated by Discovery Studio.2.1



EXPERIMENTAL SECTION

3.1. Chemistry

All commercially available solvents and reagents were used without further purification. Melting points were taken on XT-4 micro melting point apparatus and are uncorrected. Mass spectra were recorded on an electron impact ionization (EI) technique. $^1\text{H-NMR}$ and $^{13}\text{C-NMR}$ spectra were obtained on a Bruker AV-300 MHz NMR spectrometer ($^1\text{H-NMR}$ at 300 MHz, $^{13}\text{C-NMR}$ at 75 MHz) at ambient temperature. $^1\text{H-NMR}$ spectra are reported in ppm on the δ scale and referenced to the internal tetramethylsilane. The data are presented as follows: chemical shift, multiplicity (s = singlet, d = doublet, t = triplet, q = quartet, m = multiplet, br = broad, app = apparent), coupling constant(s) in Hertz (Hz), and integration. Chemical shifts (δ) were recorded relative to residual DMSO-d_6 ($\delta = 2.50$ in $^1\text{H-NMR}$ and $\delta = 35.2$ in $^{13}\text{C-NMR}$). Analytical TLC was carried out with plates precoated with silicagel 60 F_{254} (0.25 mm thick). Flash column chromatography was accomplished on silica gel 200–300 mesh. The purity of all new compounds was more than 97% which was detected by HPLC.

3.1.1. General Procedure for the synthesis of **1** and **4**

Synthesis of 7: Tryptamine (10 mmol) was mixed and stirred with trifluoroacetic acid (1 mmol) and formaldehyde (11 mmol) in refluxing acetonitrile (25 mL) for 6 h to form **7**.

Synthesis of 10: The mixture of anthranilic acid **8** (10 mmol) and triphosgene (12 mmol) was stirred in refluxing THF (50 ml) for 3 h to provide isatoic anhydride **9**, which (**9**, 10 mmol) was then coupling with **7** to give **10**.

Synthesis of 1: The mixture of **10** (10 mmol) and DDQ (10 mmol) was refluxed in $\text{ClCH}_2\text{CH}_2\text{Cl}$ (50ml) to afford rutaecarpine **1** (yield, 81%).

Synthesis of 4: Following a reduction procedure, rutaecarpine was treated with equimolar LiAlH_4 to afford the hydrogenated compound **4**.

3.1.2. General Procedure for the Preparation of **3a–g** and **5a–g**

In the presence of NaH, compounds **3a–g** and **5a–g** were prepared by stirring rutaecarpine **1** (or hydrogenated rutaecarpine **4**) with various sulphonyl chloride reagents (substituted benzenesulfonyl chloride and cyclopropanesulfonyl chloride) in DMF at room temperature. After 8–12 h, the reaction mixture was washed with water and saturated NaCl solution sequentially, dried over anhydrous Na_2SO_4 , and concentrated in vacuo. The crude products were purified by column chromatography ($\text{MeOH}/\text{CH}_2\text{Cl}_2$ 1:10 v/v) to give the targeted compounds. Characteristic data for all the synthesized compounds are as follows:

Rutaecarpine (**1**)

Pale solid; Mp 274–276°C; $^1\text{H-NMR}$ (300MHz, DMSO-d_6) δ : 2.81(m, 1H), 2.95(m, 1H), 3.20(m, 1H), 4.52(m, 1H), 6.01(s, 1H), 7.11–6.94(m, 8H), 11.26(s, 1H); $^{13}\text{C-NMR}$ (75MHz, DMSO-d_6) δ : 160.3, 146.6, 137.1, 134.3, 130.6, 128.2, 122.7, 119.8, 118.0, 116.9, 102.3, 41.7; HRMS (EI) for (M-H) $^-$: calcd 287.3153, found 287.3149;

*N*¹³-phenylsulfonyl rutaecarpine (**3a**)

Yield 67%; Pale solid; Mp 239-241°C; ¹H-NMR (300MHz, DMSO-d₆) δ: 2.85(m, 1H), 2.96(m, 1H), 3.22(m, 1H), 4.42(m, 1H), 6.01(s, 1H), 7.16-8.13(m, 13H); ¹³C-NMR (75MHz, DMSO-d₆) δ: 162.4, 149.1, 136.3, 133.5, 132.7, 130.6, 129.7, 128.3, 124.9, 119.8, 118.0, 116.9, 89.9, 41.7, 20.2; HRMS (EI) for (M+H)⁺: calcd 428.1382, found 428.1385;

*N*¹³-(4-chlorobenzenesulfonyl) rutaecarpine (**3b**)

Yield 53%; Pale solid; Mp 243-245°C; ¹H-NMR (300MHz, DMSO-d₆) δ: 2.86(m, 1H), 2.96(m, 1H), 3.20(m, 1H), 4.52(m, 1H), 6.01(s, 1H), 7.03-8.20(m, 12H); ¹³C-NMR (75MHz, DMSO-d₆) δ: 162.0, 148.8, 139.3, 136.5, 133.1, 130.6, 129.8, 129.7, 128.1, 124.9, 119.8, 118.0, 116.9, 114.5, 89.9, 41.7, 20.2; HRMS (EI) for (M+H)⁺: calcd 462.0992, found 462.0997;

*N*¹³-(4-bromobenzenesulfonyl) rutaecarpine (**3c**)

Yield 53%; Pale solid; Mp 236-238°C; ¹H-NMR (300MHz, DMSO-d₆) δ: 2.81(m, 1H), 2.85(m, 1H), 3.42(m, 1H), 3.52(m, 1H), 6.01(s, 1H), 6.98-7.93(m, 12H); ¹³C-NMR (75MHz, DMSO-d₆) δ: 161.9, 148.4, 136.5, 133.1, 132.6, 130.6, 128.1, 124.9, 119.8, 118.0, 116.8, 114.5, 89.7, 41.7, 20.3; HRMS (EI) for (M+H)⁺: calcd 506.0487, found 506.0485

*N*¹³-(4-fluorobenzenesulfonyl) rutaecarpine (**3d**)

Yield 56%; Pale solid; Mp 248-251°C; ¹H-NMR (300MHz, DMSO-d₆) δ: 2.81(m, 1H), 2.85(m, 1H), 3.41(m, 1H), 3.51(m, 1H), 5.98 (s, 1H), 6.84-7.91(m, 12H); ¹³C-NMR (75MHz, DMSO-d₆) δ: 167.9, 162.0, 148.8, 136.5, 133.4, 130.6, 129.9, 128.1, 124.9, 119.8, 118.4, 116.9, 114.5, 89.9, 41.7, 20.2; HRMS (EI) for (M+H)⁺: calcd 446.1288, found 446.1285

*N*¹³-(4-nitrobenzenesulfonyl) rutaecarpine (**3e**)

Yield 72%; Pale solid; Mp 241-242°C; ¹H-NMR (300MHz, DMSO-d₆) δ: 2.82(m, 1H), 2.86(m, 1H), 3.42(m, 1H), 3.52(m, 1H), 5.96(s, 1H), 6.94-8.14(m, 12H); ¹³C-NMR (75MHz, DMSO-d₆) δ: 162.0, 152.9, 148.8, 136.5, 130.6, 129.2, 128.1, 124.9, 119.8, 118.8, 118.0, 116.9, 114.5, 89.9, 41.7, 20.2; HRMS (EI) for (M+H)⁺: calcd 473.1233, found 473.1239

*N*¹³-(4-methylbenzenesulfonyl) rutaecarpine (**3f**)

Yield 63%; Pale solid; Mp 245-247°C; ¹H-NMR (300MHz, DMSO-d₆) δ: 2.81(m, 1H), 2.85(m, 1H), 3.42(m, 1H), 3.52(m, 1H), 5.98(s, 1H), 6.64-7.93(m, 12H); ¹³C-NMR (75MHz, DMSO-d₆) δ: 162.0, 148.8, 139.4, 136.5, 133.1, 130.4, 128.1, 127.0, 124.9, 119.8, 118.5, 116.9, 116.7, 114.5, 89.9, 41.7, 21.3, 20.2; HRMS (EI) for (M+H)⁺: calcd 442.1538, found 442.1535

*N*¹³-cyclopropanesulfonyl rutaecarpine (**3g**)

Yield 49%; Pale solid; Mp 228-230°C; ¹H-NMR (300MHz, DMSO-d₆) δ: 1.07 (m, 2H), 1.46(m, 2H), 1.72(m, 1H), 2.81(m, 1H), 2.85(m, 1H), 3.42(m, 1H), 3.52(m, 1H), 6.01(s, 1H), 7.71-6.93(m, 8H); ¹³C-NMR (75MHz, DMSO-d₆) δ: 162.0, 148.3, 136.5, 133.1, 131.5, 130.6, 128.1, 124.9, 119.8, 118.2, 117.5, 116.9, 114.5, 108.2, 89.9, 41.7, 37.5, 20.2; HRMS (EI) for (M+H)⁺: calcd 392.1382, found 392.1389

5-Methylene rutaecarpine (**4**)

Yield 76%; Pale solid; Mp 261-263°C; ¹H-NMR (300MHz, DMSO-d₆) δ: 2.81(br, 2H), 3.05(br, 2H), 3.83(m, 1H), 4.10(d, 1H), 4.80(s, 1H), 6.93-7.61(m, 8H), 8.45(s, 1H); ¹³C-NMR (75MHz, DMSO-d₆) δ: 147.1, 136.2, 135.3, 132.5, 128.1, 127.5, 123.3, 119.8, 118.4, 117.6, 111.1, 109.8, 108.2, 103.5, 57.3, 42.0, 20.7; HRMS (EI) for (M-H)⁻: calcd 273.1579, found 273.1576

*N*¹³-benzenesulfonyl-5-methylene rutaecarpine (**5a**)

Yield 76%; Pale solid; Mp 253-255°C; ¹H-NMR (300MHz, DMSO-d₆) δ: 2.85-2.87(br, 2H), 3.01(br, 2H), 3.96(m, 1H), 4.17(br, 1H), 5.02(br, 1H), 6.52-7.86 (m, 13H); ¹³C-NMR (75MHz, DMSO-d₆) δ: 147.1, 137.8, 136.5, 133.7, 129.7, 128.2, 127.5, 124.9, 121.1, 119.8, 117.6, 114.5, 110.8, 108.1, 100.5, 58.7, 42.0, 20.8; HRMS (EI) for (M+H)⁺: calcd 414.1589, found 414.1584

*N*¹³-(4-chlorobenzenesulfonyl)-5-methylene rutaecarpine (**5b**)

Yield 76%; Pale solid; Mp 249-251°C; ¹H-NMR (300MHz, DMSO-d₆) δ: 2.84-2.86(br, 2H), 3.05(m, 2H), 3.97(m, 1H), 4.12(s, 1H), 5.01(s, 1H), 6.60-7.81 (m, 12H); ¹³C-NMR (75MHz, DMSO-d₆) δ: 147.4, 139.4, 136.7, 133.1, 131.7, 129.8, 128.1, 127.5, 124.8, 121.2, 120.1, 119.2, 114.5, 109.8, 108.2, 100.6, 57.3, 43.1, 21.2; HRMS (EI) for (M+H)⁺: calcd 448.1200, found 448.1208

*N*¹³-(4-bromobenzenesulfonyl)-5-methylene rutaecarpine (**5c**)

Yield 76%; Pale solid; Mp 254-255°C; ¹H-NMR (300MHz, DMSO-d₆) δ: 2.85-2.87(br, 2H), 3.04(m, 2H), 3.97(m, 1H), 4.12(s, 1H), 5.00(s, 1H), 6.76-8.01 (m, 12H); ¹³C-NMR (75MHz, DMSO-d₆) δ: 147.2, 137.0, 136.1, 133.1, 132.3, 128.1, 127.3, 124.9, 121.1, 120.2, 118.8, 114.5, 109.6, 108.2, 100.3, 57.7, 42.0, 20.8; HRMS (EI) for (M+H)⁺: calcd 492.0694, found 492.0697

*N*¹³-(4-fluorobenzenesulfonyl)-5-methylene rutaecarpine (**5d**)

Yield 76%; Pale solid; Mp 267-269°C; ¹H-NMR (300MHz, DMSO-d₆) δ: 2.85-2.87(br, 2H), 3.04(m, 2H), 3.97(m, 1H), 4.12(s, 1H), 5.00(s, 1H), 6.71-7.87 (m, 12H); ¹³C-NMR (75MHz, DMSO-d₆) δ: 168.1, 146.9, 136.3, 133.4, 128.1, 127.5, 124.9, 121.1, 119.8, 118.4, 114.5, 109.8, 108.2, 100.1, 42.0, 20.7, HRMS (EI) for (M+H)⁺: calcd 432.1495, found 432.1493

*N*¹³-(4-nitrobenzenesulfonyl)-5-methylene rutaecarpine (**5e**)

Yield 76%; Pale solid; Mp 253-255°C; ¹H-NMR (300MHz, DMSO-d₆) δ: 2.84-2.86(br, 2H), 3.05(m, 2H), 4.02(m, 1H), 4.11(s, 1H), 5.06(s, 1H), 6.86-8.42 (m, 12H); ¹³C-NMR (75MHz, DMSO-d₆) δ: 154.3, 148.2, 137.0, 135.9, 130.2, 128.1, 126.8, 124.9, 121.1, 118.7, 114.5, 113.1, 109.8, 106.5, 100.1, 42.0, 20.7; HRMS (EI) for (M+H)⁺: calcd 459.1440, found 459.1446

*N*¹³-(4-methylbenzenesulfonyl)-5-methylene rutaecarpine (**5f**)

Yield 76%; Pale solid; Mp 252-254°C; ¹H-NMR (300MHz, DMSO-d₆) δ: 2.34(s, 3H), 2.85-2.87(br, 2H), 3.01(br, 2H), 3.96(m, 1H), 4.17(br, 1H), 5.02(br, 1H), 6.60-7.80 (m, 12H); ¹³C-NMR (75MHz, DMSO-d₆) δ: 147.1, 139.4, 136.5, 133.1, 130.0, 128.6, 127.5, 121.8, 120.3, 118.2, 114.7, 110.9, 108.7, 100.9, 41.9, 22.7, 20.6; HRMS (EI) for (M+H)⁺: calcd 428.1746, found 428.1745

*N*¹³-cyclopanesulfonyl-5-methylene rutaecarpine (**5g**)

Yield 76%; Pale solid; Mp 235-236°C; ¹H-NMR (300MHz, DMSO-d₆) δ: 1.07 (m, 2H), 1.46(m, 2H), 1.72(m, 1H), 2.81(br, 2H), 3.05(br, 2H), 3.83(m, 1H), 4.10(d, 1H), 4.80(s, 1H), 6.93-7.61(m, 8H), 8.45(s, 1H); ¹³C-NMR (75MHz, DMSO-d₆) δ: 146.3, 136.5, 133.1, 131.5, 128.1, 123.3, 119.8, 118.4, 117.6, 111.1, 109.8, 108.2, 103.5, 57.3, 44.6, 41.7, 37.5, 20.2; HRMS (EI) for (M+H)⁺: calcd 378.1589, found 378.1583

3.2 Cytotoxicity

3.2.1 Cell culture

Five human cancer cell lines including A549, HepG-2, U251, HeLa and MCF-7 were obtained from Cancer Cell Repository (Shanghai cell bank). Cells were maintained in DMEM medium or RPMI-1640 medium (Gibco, USA) supplemented with 10% (v/v) heat-inactivated fetal bovine serum, antibiotics (100 U/ml penicillin and 100 U/ml streptomycin), at 37°C in a humidified atmosphere of 5% CO₂.

3.2.2 *In vitro* anti-proliferation assay

Cells were plated in 96-well culture plates at an initial density of 4×10³ viable cells per well in 96-well plates. After 24 h growth, various concentrations of tested compounds were respectively applied to the cells. Cell viability was estimated by measuring the metabolism of MTT. Briefly, 100 μL of MTT solution (1 mg/mL) was added to each well of a 96-well plate, and cells were maintained for 4 h at 37°C. The medium was aspirated and the formazan contained in cells was solubilized by 100 μL of DMSO for 1 h. The absorbance was measured at 570 nm by a plate reader (Spectra MAX 190, Molecular Devices Corporation). The inhibition rate was calculated as follows:

$$\text{Inhibition Rate} = (1 - \text{OD}_{570} \text{ drug treated} / \text{OD}_{570} \text{ control}) \times 100$$

IC₅₀ values were determined graphically from the growth inhibition curves obtained after a 48 h exposure of the cells to tested compounds, using the software from Zhenzhou University.

3.3 *In Vivo* antitumor activity assay with **3d**

Female ICR mice, purchased from The Experimental Animal Center of Zhenzhou University, were maintained on a standard diet and water made freely available in a conventional animal colony. The mice were 6-8 weeks old at the beginning of the experiment. The tumor used was HepS that forms solid tumors when injected subcutaneously. HepS cells for initiation of subcutaneous tumors were obtained from the ascitic form of the tumors in mice, which were serially transplanted once per week. Subcutaneous tumors were implanted by injecting 0.2 mL of normal saline solution containing 1×10⁷ viable tumor cells under the skin on the right oter. Twenty-four hours after implantation, the tumor-bearing mice were randomly assigned into five experimental groups (10 per group). The mice were given a daily intraperitoneal injection of CPT (positive control) and intragastric administration of **3d** (20 mg/kg, 40 mg/kg and 80 mg/kg) pre-dissolved in 4% Tween 80 in normal saline solution, for nine consecutive days; and the vehicle

alone was used as the negative control. Twenty-four hours after the last administration, animal welfare and experimental procedures were carried out strictly in accordance with the Guide for the Care and Use of Laboratory Animals (The Ministry of Science and Technology of China, 2006) and the related ethical regulations of our university. Every effort was made to minimize animals' suffering and to reduce the number of animals used.

The tumor wet weights of the treated (Tw) and control (Cw) groups were measured on the last day of each experiment and the percentage of tumor growth inhibition was calculated as follows^[27]:

$$\text{Inhibition (\%)} = [1 - (T_w/C_w)] \times 100$$

Observations were also made to assess the toxicity of **3d** on thymus and spleen.

3.3 *in silico* molecular docking

3.3.1 Structure validation

The discovery of novel TopoI inhibitors is facilitated by the improvement of a variety of biochemical and cellular assays and X-ray crystal structures. The X-ray crystal structure of human TopoI-DNA complex bound with camptothecin (PDB code 1T8I) was selected for hit identification in this work

3.3.2 Docking, scoring, and interaction energy study

The structures of synthetic compounds and the control, rutaecarpine, were prepared using ChemOffice 2005 and optimized with MM2 force field. The docking study was performed using LigandFit with CHARMM force field (Discovery Studio 2.1). The camptothecin in TopoI-DNA complex crystal structure generated the read-made active site of TopoI. The top 10 conformations were generated based on the DockScore value after the energy minimization using smart minimizer method. The evaluation for ligand binding affinity was performed by scoring functions, including Piecewise Linear Potential and DockScore. The equation of DockScore is given as follows:

$$\text{DockScore (forcefield)} = - (E_{\text{interaction (ligand/receptor)}} + E_{\text{internal (ligand)}})$$

The conformations of ligands were estimated and prioritized by the DockScore function. The interaction energy in above-mentioned equation stands for the sum of the van der Waals energy and electrostatic energy. The grid-base evaluation of interaction was performed because of the time-consuming problem.

The PLP scoring function, including PLP1 and PLP2, correlates well to ligand binding affinities. Higher PLP value indicates the larger pK_i value. In the PLP1 and PLP2 function, each non-hydrogen atom of the ligand and the receptor is assigned a PLP atom type. Besides, an atomic radius is assigned to each atom, except by hydrogen in PLP2 function. To calculate the interaction energy, the ligand/receptor complex with the highest DockScore was initially energy-minimized with harmonic restraint under Adopted Basis Newton-Raphson (ABNR) method. The calculation of the interaction energy was given as follows:

$$E_{\text{interaction}} = E_{\text{complex}} - (E_{\text{ligand}} + E_{\text{receptor}})$$

where the energy was calculated under the CHARMM force field.

CONCLUSION

Two series of novel sulfonic rutaecarpine esters were synthesized and tested for anti-proliferative activity against five human cancer cell lines by the *in vitro* MTT assay. The preliminary SAR of the synthetic compounds was concluded based on the obtained cytotoxic data. Among them, compound **3d** exhibited the most potent anti-tumor activity against all test cell lines. Gratifyingly, **3d** exhibited an excellent *in vivo* antitumor profile (i.e. high efficacy and low side-effect) in HepS xenograft model as compared to CPT. According to *in silico* molecular docking, seven hits **3a-3g** were identified to possess both *in vitro* antitumor activity and potential TopoI inhibitory activity. Although no docking formation was observed according to there was no hydrogen bond between the ligand (**4** and **5a-5g**) and the important residues of TopoI, **5a-5g** still exhibited cytotoxicity against different tested cell lines. This phenomenon indicated other interactions might exist between the ligand and the active site of TopoI besides intermolecular H-bonds. Further research on the structure modification of rutaecarpine is currently in progress in our lab.

REFERENCES

- [1] Y. H. Hsiang, R. Hertzberg, S. Hecht and L. Liu, *J. Biol. Chem.* **1985**, 260, 14873-14878.

- [2] O. Lavergne, L. Lesueur-Ginot, F. P. Rodas, P. G. Kasprzyk, J. Pommier, D. Demarquay, G. Prévost, G. Ulibarri, A. Rolland and A. M. Schiano-Liberatore, *J. Med. Chem.* **1998**, *41*, 5410-5419.
- [3] W. ten Bokkel Huinink, M. Gore, J. Carmichael, A. Gordon, J. Malfetano, I. Hudson, C. Broom, C. Scarabelli, N. Davidson and M. Spanczynski, *J. Clin. Oncol.* **1997**, *15*, 2183-2193.
- [4] L. B. Saltz, J. V. Cox, C. Blanke, L. S. Rosen, L. Fehrenbacher, M. J. Moore, J. A. Maroun, S. P. Ackland, P. K. Locker and N. Pirota, *N. Engl. J. Med.* **2000**, *343*, 905-914.
- [5] Z. Mi and T. G. Burke, *Biochemistry* **1994**, *33*, 10325-10336.
- [6] a) L. P. Rivory and J. Robert, *Pharmacol. Ther.* **1995**, *68*, 269-296; b) Y. G. Pommier, J. Barceló, T. Furuta, H. Takemura, O. Sordet and Z. Y. Liao, *Camptothecins in cancer therapy* **2005**, 61-107.
- [7] a) M. Kim, H. Turnquist, J. Jackson, M. Sgagias, Y. Yan, M. Gong, M. Dean, J. G. Sharp and K. Cowan, *Clin. Cancer Res.* **2002**, *8*, 22-28; b) K. Nakatomi, M. Yoshikawa, M. Oka, Y. Ikegami, S. Hayasaka, K. Sano, K. Shiozawa, S. Kawabata, H. Soda and T. Ishikawa, *Biochem. Biophys. Res. Commun.* **2001**, *288*, 827-832.
- [8] a) D. Abigeres, J. P. Armand, G. G. Chabot, L. Da Costa, E. Fadel, C. Cote, P. Hérait and D. Gandia, *J. Nat. Cancer Inst.* **1994**, *86*, 446-449; b) W. J. Slichenmyer, E. K. Rowinsky, R. C. Donehower and S. H. Kaufmann, *J. Nat. Cancer Inst.* **1993**, *85*, 271-291.
- [9] J. E. Chrencik, B. L. Staker, A. B. Burgin, P. Pourquier, Y. Pommier, L. Stewart and M. R. Redinbo, *J. Mol. Biol.* **2004**, *339*, 773-784.
- [10] a) E. Kiselev, N. Empey, K. Agama, Y. Pommier and M. Cushman, *J. Org. Chem.* **2012**, *77*, 5167-5172; b) T. X. Nguyen, A. Morrell, M. Conda-Sheridan, C. Marchand, K. Agama, A. Bermingam, A. G. Stephen, A. Chergui, A. Naumova and R. Fisher, *J. Med. Chem.* **2012**, *55*, 4457-4478; c) G. L. Beretta, V. Zuco, P. Perego and N. Zaffaroni, *Curr. Med. Chem.* **2012**, *19*, 1238-1257.
- [11] M. Goldberg and D. Robertson, *Pharmacol. Rev.* **1983**, *35*, 143-180.
- [12] O. Heinonen, S. Shapiro, L. Tuominen and M. Turunen, *The Lancet* **1974**, *304*, 675-677.
- [13] P. L. Yu, H. L. Chao, S. W. Wang and P. S. Wang, *J. Cell. Biochem.* **2009**, *108*, 469-475.
- [14] H. C. Ko, Y. H. Wang, K. T. Liou, C. M. Chen, C. H. Chen, W. Y. Wang, S. Chang, Y. C. Hou, K. T. Chen and C. F. Chen, *Euro. J. Pharmacol.* **2007**, *555*, 211-217.
- [15] a) Y. C. Huang, J. H. Guh and C. M. Teng, *Life sci.* **2004**, *75*, 35-49; b) X. F. Fei, B. X. Wang, T. J. Li, S. Tashiro, M. Minami, D. J. Xing and T. Ikejima, *Cancer Sci.* **2003**, *94*, 92-98.
- [16] Y. Takada, Y. Kobayashi and B. B. Aggarwal, *J. Biol. Chem.* **2005**, *280*, 17203-17212.
- [17] a) W. F. Chiou, C. J. Chou, A. Y. C. Shum and C. F. Chen, *Euro. J. Pharmacol.* **1992**, *215*, 277-283; b) W. F. Chiou, C. J. Chou, J. F. Liao, A. Y. C. Sham and C. F. Chen, *Euro. J. Pharmacol.* **1994**, *257*, 59-66.
- [18] Y. Zhang, Q. H. Zhang, L. J. Wu, S. I. Tashiro, S. Onodera and T. Ikejima, *J. Asian Nat. Prod. Res.* **2004**, *6*, 19-27.
- [19] a) J. Jiang and C. Hu, *Molecules* **2009**, *14*, 1852-1859; b) S. F. Kan, C. H. Yu, H. F. Pu, J. M. Hsu, M. J. Chen and P. S. Wang, *J. Cell. Biochem.* **2007**, *101*, 44-56.
- [20] a) H. Sun, Y. Liu, Y. Huang, S. Pan, D. Huang, J. Guh, F. Lee, S. Kuo and C. Teng, *Oncogene* **2007**, *26*, 3941-3951; b) S. C. Gupta, C. Sundaram, S. Reuter and B. B. Aggarwal, *BBA-Gene Regulatory Mechanisms* **2010**, *1799*, 775-787.
- [21] S. F. Kan, W. J. Huang, L. C. Lin and P. S. Wang, *Int. J. Cancer* **2004**, *110*, 641-651.
- [22] H. Lin, S. C. Tsai, J. J. Chen, Y. C. Chiao, S. W. Wang, G. J. Wang, C. F. Chen and P. S. Wang, *Metabolism* **1999**, *48*, 1532-1535.
- [23] J. Yang, L. J. Wu, S. I. Tashiro, S. Onodera and T. Ikejima, *Free Radical Res.* **2008**, *42*, 492-504.
- [24] G. Dong, C. Sheng, S. Wang, Z. Miao, J. Yao and W. Zhang, *J. Med. Chem.* **2010**.
- [25] a) Z. H. Wang, W. Y. Li, F. L. Li, L. Zhang, W. Y. Hua, J. C. Cheng and Q. Z. Yao, *Chin. Chem. Lett.* **2009**, *20*, 542-544; b) Z. H. Wang, Y. Dong, T. Wang, M. H. Shang, W. Y. Hua and Q. Z. Yao, *Chin. Chem. Lett.* **2010**, *21*, 297-300.
- [26] a) T. Kametani, T. Higa, C. Van Loc, M. Ihara, M. Koizumi and K. Fukumoto, *J. Am. Chem. Soc.* **1976**, *98*, 6186-6188; b) T. Kametani, T. Higa, K. Fukumoto and M. Koizumi, *Heterocycles* **1976**, *4*, 23-28.
- [27] J. Wu, C. Li, M. Zhao, W. Wang, Y. Wang and S. Peng, *Bioorgan. Med. Chem.* **2010**, *18*, 6220-6229.